PHYSICAL REVIEW B **78**, 140407(R) (2008)

Importance of stacking to the collinear magnetic phases of the geometrically frustrated antiferromagnet $CuFeO_2$

R. S. Fishman,[1] F. Ye,[2] J. A. Fernandez-Baca,[2,3] J. T. Haraldsen,[1] and T. Kimura[4]
[1]*Materials Science and Technology Division, Oak Ridge National Laboratory, Oak Ridge, Tennessee 37831, USA*
[2]*Neutron Scattering Science Division, Oak Ridge National Laboratory, Oak Ridge, Tennessee 37831, USA*
[3]*Department of Physics and Astronomy, The University of Tennessee, Knoxville, Tennessee 37831, USA*
[4]*Division of Materials Physics, Graduate School of Engineering Science, Osaka University, Toyanaka, Osaka, 560-8531, Japan*
(Received 21 August 2008; published 28 October 2008)

The correct stacking of hexagonal layers is used to obtain accurate estimates for the exchange and anisotropy parameters of the geometrically frustrated antiferromagnet $CuFeO_2$. Those parameters are highly constrained by the stability of a collinear metamagnetic phase between fields of 13.5 and 20 T. Constrained fits of the spin-wave frequencies of the collinear $\uparrow\uparrow\downarrow\downarrow$ phase below 7 T are used to identify the magnetic unit cell of the metamagnetic $\uparrow\uparrow\uparrow\downarrow\downarrow$ phase, which contains two hexagonal layers and 10 Fe^{3+} spins.

DOI: 10.1103/PhysRevB.78.140407 PACS number(s): 75.30.Ds, 75.50.Ee, 61.05.fg

Because of their rich magnetic phase diagrams, geometrically frustrated antiferromagnets have long occupied an important place in condensed-matter physics.[1] The antiferromagnetic interactions between the Fe^{3+} spins of $CuFeO_2$ are geometrically frustrated within each hexagonal plane since no spin configuration can simultaneously minimize the coupling energies of all three neighbors around an equilateral triangle. Unlike for many geometrically frustrated antiferromagnets, quantum fluctuations about the magnetic ground states of $CuFeO_2$ can be safely neglected due to the large $S=5/2$ spins. Whereas geometric frustration often leads to magnetic phases with noncollinear spins and complex unit cells, magnetic anisotropy perpendicular to the hexagonal planes in $CuFeO_2$ produces two different collinear magnetic phases. The $\uparrow\uparrow\downarrow\downarrow$ phase[2,3] sketched in Fig. 1(a) is stable up to the field $B_{c1}\approx 7$ T. Between $B_{c2}\approx 13.5$ T and $B_{c3}\approx 20$ T, another collinear phase with a net moment of $1\mu_B$ per Fe^{3+} ion[4,5] has been assumed to resemble the $\uparrow\uparrow\uparrow\downarrow\downarrow$ phase shown in Fig. 2 for type B stacking, with 5 spins per unit cell. Incommensurate and noncollinear phases were identified between B_{c1} and B_{c2} and above B_{c3}.[4,5]

Previous efforts to understand the collinear magnetic phases[3,6] and to estimate the exchange and anisotropy parameters[7] of $CuFeO_2$ assumed that the hexagonal layers were stacked sequentially on top of each other. In the presence of spin-phonon coupling, a metamagnetic phase with five sublattices (SLs) can also be produced by classical spins in isolated two-dimensional layers with nearest-neighbor exchange.[8] We now demonstrate that an accurate determination of the Heisenberg parameters must employ the correct stacking of hexagonal layers. We also show that the stability of a metamagnetic phase between B_{c2} and B_{c3} (Refs. 4 and 5) strongly constrains those parameters. Whereas earlier work[7] assuming a sequential stacking was unable to explain the observed spin-wave (SW) frequencies of the zero-field twins, realistic magnetic stackings are now used to explain all features of the low-field collinear phase and to identify the magnetic unit cell of the high-field collinear phase in $CuFeO_2$.

The observation of collinear magnetic phases that are fully polarized along the $\pm\hat{\mathbf{z}}$ directions at low temperatures led to the assumption[3,6] that the Fe^{3+} spins were "Ising-like." However, measurements of the zero-field SW frequencies[7,9] plotted in Fig. 1(b) reveal SW gaps of only about 0.9 meV at wave vectors $(H,H,L=\frac{3}{2})$ with $H=0.21$ and 0.29, on either side of the ordering wave vector $\mathbf{Q}=(\frac{1}{4},\frac{1}{4},\frac{3}{2})$. If the spins were truly "Ising-like," then the SW frequencies would be much higher and they would not exhibit a significant dispersion along the $(0,0,L)$ direction[7,10] perpendicular to the hexagonal planes. With little change in wave vectors, the SW gaps are reduced either by an applied field along the $\hat{\mathbf{z}}$ direction or by the substitution of nonmagnetic Al^{3+} ions for Fe^{3+}. Above the field B_{c1} (Refs. 4 and 5) or an Al concentration of about 1.6%,[9] the SW gaps vanish, the magnetic ground state becomes noncollinear, and the crystals display multiferroic behavior.[11–13]

Assuming that the hexagonal planes stack sequentially, we recently fit[7] the SW frequencies of pure $CuFeO_2$ to the predictions of the Heisenberg model

$$H=-\frac{1}{2}\sum_{i\neq j}J_{ij}\mathbf{S}_i\cdot\mathbf{S}_j-D\sum_i S_{iz}^2-2\mu_B B\sum_i S_{iz}, \qquad (1)$$

which includes single-ion anisotropy D and a magnetic field B. Anisotropy can arise either from the low-spin states of Fe^{3+} (Ref. 14) or ionic defects.[15] For "Ising-like" spins, D would be much greater than the exchange parameters J_{ij}. In a further simplification, we ignored the very small ($<0.4\%$) distortion of the hexagonal plane[5,16] below the Néel temperature, which can produce only a very small change in the exchange parameters and hence in the SW frequencies. Despite these simplifications, the SW dispersions evaluated along the $(H,H,\frac{3}{2})$ and $(0,0,L)$ axes agree quite well with inelastic neutron-scattering measurements.[7] However, we were unable to fit the frequency of the two twins with wave vectors rotated $\pm\pi/3$ away from $\mathbf{Q}$ in the $(H,K,\frac{3}{2})$ plane. Without attempting to fit the twins, we obtained the exchange and anisotropy parameters given in line i of Table I, where J_{pm} or J_{zm} are the mth nearest-neighbor exchange parameters within each hexagonal plane or between adjacent planes.

To better understand the metamagnetic phase between B_{c2} and B_{c3}, we have recalculated the SW frequencies of the

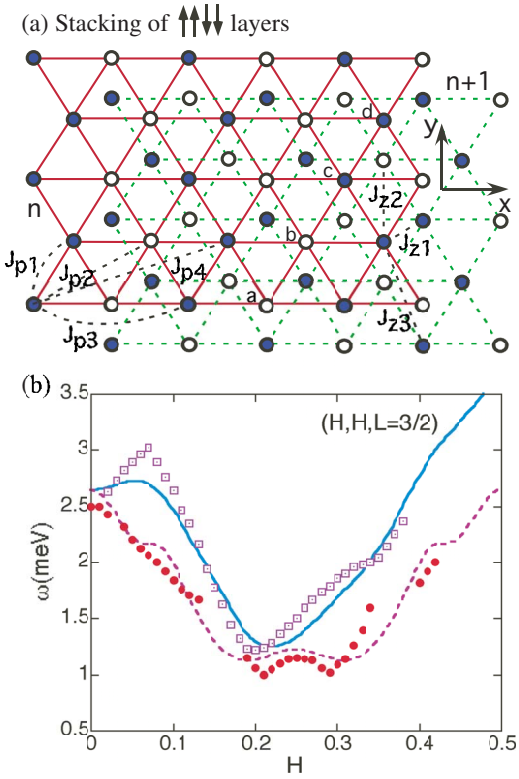

FIG. 1. (Color online) (a) The low-field spin configuration (up spins are empty and down spins are filled circles) in each hexagonal plane with the four inequivalent spins a, b, c, and d. Both the n (solid) and $n+1$ (dashed) layers are shown with the exchange parameters indicated. (b) The fit of the SW frequencies along the $(H,H,\frac{3}{2})$ axis using the exchange and anisotropy parameters given in line iii of Table I. Open squares give the frequencies of the twins and solid circles give the frequencies of the main SW branch with ordering wave vector at $H=\frac{1}{4}$.

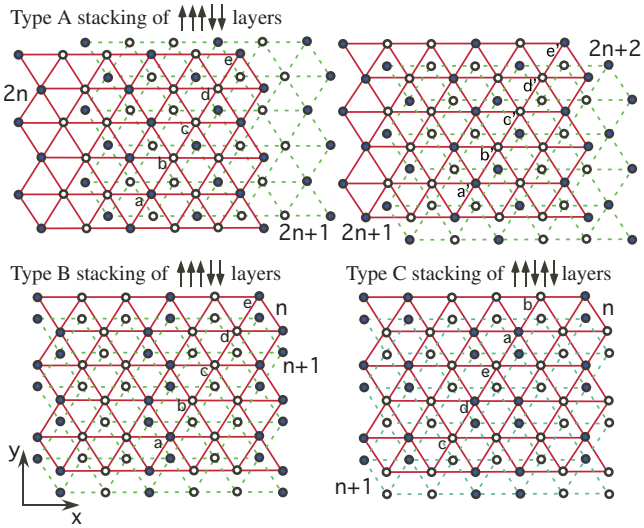

FIG. 2. (Color online) Three types of magnetic stacking that satisfy the conditions for local stability of the metamagnetic phase. In type A stacking, the stacking patterns on the left and right alternate.

TABLE I. Heisenberg parameters of $CuFeO_2$ obtained from fits of the zero-field SW frequencies. Line i assumes sequential stacking of the hexagonal layers (Ref. 7), ii and iii use the realistic stacking in Fig. 1(a) while iii also constrains the parameters stabilizing the collinear phase between B_{c2} and B_{c3}. Exchange and anisotropy parameters are in meV, T_N^{MF} is in kelvin.

fit	J_{p1}	J_{p2}	J_{p3}	J_{p4}	J_{z1}	J_{z2}	J_{z3}	D	T_N^{MF}
i	−0.46	−0.20	−0.26		−0.13	0.00		0.07	46
ii	−0.75	−0.17	−0.10	0.01	−0.51	−0.19	−0.06	0.14	65
iii	−0.23	−0.12	−0.16	0.00	−0.06	0.07	−0.05	0.22	25

$\uparrow\uparrow\downarrow\downarrow$ phase below B_{c1} using the realistic magnetic stacking of the hexagonal layers shown in Fig. 1(a) where the displacement of layer $n+1$ from layer n is $\mathbf{d}=\hat{\mathbf{x}}+2\hat{\mathbf{y}}/\sqrt{3}$ (lattice constant set to one). All other stackings of the $\uparrow\uparrow\downarrow\downarrow$ layers have higher coupling energies. Because spins a, b, c, or d experience the same local environment on every layer, the magnetic unit cell still contains only 4 SLs. The first few exchange pathways J_{pm} and J_{zm} are indicated in Fig. 1(a).

The SW frequencies are evaluated using a Holstein-Primakoff $1/S$ expansion about the classical limit. On the spin-up a and b sites, we replace $S_{iz}=S-\alpha_i^\dagger\alpha_i$, $S_i^+=S_{ix}+iS_{iy}=\sqrt{2S}\alpha_i$, and $S_i^-=S_{ix}-iS_{iy}=\sqrt{2S}\alpha_i^\dagger$ ($\alpha_i=a_i$ or b_i). On the spin-down c and d sites, we replace $S_{iz}=-S+\gamma_i^\dagger\gamma_i$, $S_i^+=\sqrt{2S}\gamma_i^\dagger$, and $S_i^-=\sqrt{2S}\gamma_i$ ($\gamma_i=c_i$ or d_i). The SW frequencies $\omega_{\mathbf{k}}$ at wave vector $\mathbf{k}$ are then obtained by solving the equations of motion for the vectors $\mathbf{v}_{\mathbf{k}}=(a_{\mathbf{k}},b_{\mathbf{k}},c_{\mathbf{k}}^\dagger,d_{\mathbf{k}}^\dagger)$ and $\mathbf{v}_{\mathbf{k}}^\dagger$. The equation of motion for $\mathbf{v}_{\mathbf{k}}$ may be written in terms of the 4×4 matrix $\underline{M}(\mathbf{k})$ as $id\mathbf{v}_{\mathbf{k}}/dt=-[H,\mathbf{v}_{\mathbf{k}}]=\underline{M}(\mathbf{k})\mathbf{v}_{\mathbf{k}}$ with SW frequencies given by the condition $\mathrm{Det}[\underline{M}(\mathbf{k})-\omega_{\mathbf{k}}\underline{I}]=0$. Only positive frequencies $\omega_{\mathbf{k}}\geq0$ are retained.

As expected for a collinear antiferromagnet and shown schematically for any wave vector in Fig. 3(a), each of the SW branches is linearly split by a magnetic field. The lowest SW frequency with wave vector (0.21,0.21,1.5) or (0.29,0.29,1.5) will vanish at the field $0.9\ \mathrm{meV}/2\mu_B\approx7.7$ T, which is slightly larger than B_{c1}. With the correct stacking of the hexagonal layers, the parameters in line ii of Table I are obtained by fitting the SW frequencies of the main branches along the $(H,H,\frac{3}{2})$ and $(0,0,L)$ axes as well

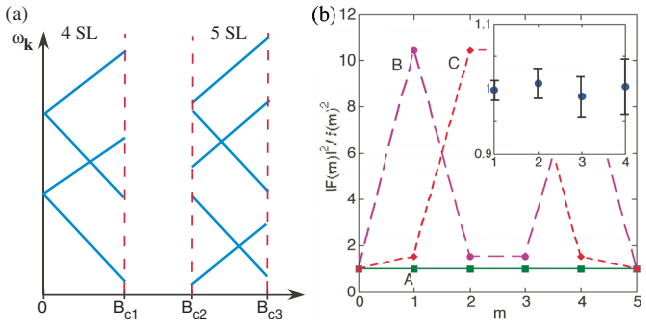

FIG. 3. (Color online) (a) Schematic field dependence of the SW frequencies $\omega_{\mathbf{k}}^{(s)}$ in 4 or 5 SL phases. (b) The predicted, normalized elastic intensities $|F(m)|^2/f(m)^2$ versus m [$H=\frac{m}{5}$ along the $(H,H,0)$ axis] for stackings A–C. The inset are the experimental, normalized intensities versus m.

as the SW frequencies of the twins evaluated along $(H,H,\frac{3}{2})$.

Several possible collinear metamagnetic phases carry a net moment of $1\mu_B$ per Fe^{3+} ion and exhibit elastic peaks at wave vectors $(\frac{m}{5},\frac{m}{5},0)$ in the $L=0$ basal plane.[4] Two configurations are possible in each hexagonal plane: the $\uparrow\uparrow\uparrow\downarrow\downarrow$ pattern sketched in the lower left of Fig. 2 and the $\uparrow\uparrow\downarrow\uparrow\downarrow$ pattern sketched in the lower right. Depending on the stacking, the magnetic unit cell of the metamagnetic phase may contain either five or ten magnetic ions. For example, type A stacking of $\uparrow\uparrow\uparrow\downarrow\downarrow$ layers in Fig. 2 contains 10 SLs while type B stacking of $\uparrow\uparrow\uparrow\downarrow\downarrow$ layers and type C stacking of $\uparrow\uparrow\downarrow\uparrow\downarrow$ layers contain 5 SLs. In type A stacking with displacements $\mathbf{d}=-\hat{\mathbf{x}}-\hat{\mathbf{y}}/\sqrt{3}$ (layers $2n$ to $2n+1$) and $\mathbf{d}'=\hat{\mathbf{x}}+2\hat{\mathbf{y}}/\sqrt{3}$ (layers $2n+1$ to $2n+2$), the local environments of spin α on even layers and spin α' on odd layers are different: a is coupled by J_{z1} to three up spins on layer $2n+1$ while a' is coupled by J_{z1} to two up spins and one down spin on layer $2n+2$. In both type B and C stackings, the displacement vector is $\mathbf{d}=-\hat{\mathbf{y}}/\sqrt{3}$.

Two conditions must be satisfied for the local stability of a metamagnetic phase. First, the SW frequencies $\omega_{\mathbf{k}}^{(s)}$ must all be real for every $\mathbf{k}$. This condition is independent of the magnetic field, which only shifts the frequencies by $\pm 2\mu_B B$. Second, the SW weights $W_{\mathbf{k}}^{(s)}$ that appear as coefficients of the delta functions in the spin-spin correlation function,

$$S(\mathbf{k},\omega)=\frac{1}{N}\int dt e^{-i\omega t}\sum_{i,j} e^{i\mathbf{k}\cdot(\mathbf{R}_j-\mathbf{R}_i)}\{\langle S_i^+ S_j^-(t)\rangle+\langle S_i^- S_j^+(t)\rangle\}$$
$$=\sum_s W_{\mathbf{k}}^{(s)}\delta(\omega-\omega_{\mathbf{k}}^{(s)}), \qquad (2)$$

must all be positive. Those weights are most easily evaluated by expanding $S(\mathbf{k},\omega)$ within the HP formalism and then solving the equations of motion for the spin Green's functions.

An apparently equivalent but much easier way to guarantee that the weights $W_{\mathbf{k}}^{(s)}$ are positive is to examine the field dependence of the SW frequencies. For a stable 5 SL collinear phase, three of the 5 SW modes must linearly increase with field while two must linearly decrease, as shown in Fig. 3(a). For a stable 10 SL collinear phase, six of the 10 SW modes must linearly increase and four must linearly decrease with field. If this condition is violated for any $\mathbf{k}$, then some of the weights $W_{\mathbf{k}}^{(s)}$ are found to be negative and the phase is unstable. Of course, the softening of any SW branch with field signals the local instability of that metamagnetic phase.

Unfortunately, the exchange and anisotropy parameters given by lines i and ii of Table I do not satisfy both conditions for the local stability of any possible stacking of $\uparrow\uparrow\uparrow\downarrow\downarrow$ or $\uparrow\uparrow\downarrow\uparrow\downarrow$ layers between the fields B_{c2} and B_{c3}. In other words, fits to the SW frequencies of the zero-field $\uparrow\uparrow\downarrow\downarrow$ phase are inconsistent with the existence of a collinear metamagnetic phase.

This inconsistency may be eliminated by fitting the zero-field SW frequencies of the $\uparrow\uparrow\downarrow\downarrow$ phase while simultaneously constraining the exchange and anisotropy parameters to stabilize a metamagnetic phase between B_{c2} and B_{c3}. Note that this constraint utilizes only the observed stability of the metamagnetic phase over a range of magnetic fields and not the measured SW frequencies of that phase. The three phases shown in Fig. 2 are the only ones that satisfy both conditions for local stability when the exchange and anisotropy parameters are obtained from constrained zero-field fits of the SW frequencies. A constrained fit assuming one of the three stackings in Fig. 3 produces fitting parameters that give higher energies for the other two possible stackings.

To determine which of these three phases is actually observed, we evaluate the magnetic structure factor $F(m)$ for the elastic peaks in the $L=0$ basal plane at wave vectors $(H,H,0)$ with $H=m/5$. In terms of the Fe^{3+} magnetic form factor $f(m)$, $F(0)=f(0)$ for all three possible phases. The normalized intensities $|F(m)|^2/f(m)^2$ are plotted versus m in Fig. 3(b). When the magnetic moments of six adjacent layers are summed, stacking A produces the pattern $0\uparrow 000$ along $\hat{\mathbf{x}}$ so that $|F^A(m)|^2/f(m)^2=1$ is constant. If left or right stacking pattern in the top panel of Fig. 2 were continued indefinitely rather than alternating, then the resulting phase would have no elastic peaks in the $L=0$ basal plane. The layer sums of stackings B or C produce $\uparrow\uparrow\uparrow\downarrow\downarrow$ or $\uparrow\uparrow\downarrow\uparrow\downarrow$ patterns along $\hat{\mathbf{x}}$, causing $|F(m)|^2/f(m)^2$ to change by a factor of 10.5 as m increases from one to two.

For comparison, the experimental results[4,11] for the elastic intensities are plotted in the inset of Fig. 3(b). The normalized intensity $|F(m)|^2/f(m)^2$ for $m=1-4$ is constant to within about 1%. Therefore, only type A stacking of $\uparrow\uparrow\uparrow\downarrow\downarrow$ layers with a 10 SL unit cell is possible. An alternative 10 SL stacking of $\uparrow\uparrow\downarrow\uparrow\downarrow$ layers can produce the same elastic intensity in the $(H,H,0)$ direction as the preferred type A stacking of $\uparrow\uparrow\uparrow\downarrow\downarrow$ layers. Consequently, the observed $(H,H,0)$ elastic peaks alone are insufficient to fix the magnetic configuration of the metamagnetic phase.

The exchange and anisotropy parameters associated with stacking A are given on line iii of Table I. As in our original fits,[7] $|J_{p3}|>|J_{p2}|$ but J_{p4} is negligible. Since J_{z3} is comparable to J_{z1}, even longer-ranged interactions between neighboring planes might exist. All of the interactions J_{zm} between adjacent planes are much smaller in magnitude than the interactions J_{pm} $(m<4)$ within a plane. Using these parameters, the fits of the main and twin SW branches are plotted along the $(H,H,\frac{3}{2})$ axis in Fig. 1(b).

Constraining the fits of the zero-field SW frequencies to produce a stable metamagnetic phase has a substantial effect on the exchange and anisotropy parameters. For example, J_{p1} is reduced by about 70% from line ii to line iii of Table I. While a wide range of parameters can provide reasonable fits to the zero-field SW data, demanding that a metamagnetic phase is stabilized between B_{c2} and B_{c3} considerably narrows the possible range of those parameters. Also notice that the mean-field transition temperature T_N^{MF} listed in line iii of Table I is much closer to the measured transition temperature of 14 K (Ref. 4) between partially disordered and paramagnetic phases than the transition temperatures of the unconstrained fits in lines i and ii. Of all three fits, line iii produces a crystal-field environment that is most "Ising-like," with the anisotropy D about the same size as the nearest-neighbor exchange J_{p1}. The difference between the parameters in lines

i–iii of Table I underscores the danger of using even an extensive set of SW measurements for a single magnetic phase to fix the parameters of a Heisenberg model.

Surprisingly, the high-field collinear phase is the 10 SL phase sketched in Fig. 2 rather than the 5 SL phase that had been previously assumed.[4,5] Projected onto the $(H,H,0)$ axis, this 10 SL phase agrees with the metamagnetic phase conjectured by Mitsuda *et al.*[4] Because it remains locally stable up to about 34.5 T (very close to the critical field B_{c4} measured by Terada *et al.*[5]), the disappearance of the 10 SL $\uparrow\uparrow\uparrow\downarrow\downarrow$ phase at B_{c3} probably occurs at a first-order transition between collinear and noncollinear phases. That appears to be the case for the $\uparrow\uparrow\downarrow\downarrow$ phase since B_{c1} is lower than the 7.7 T field where the SW gap would vanish and the $\uparrow\uparrow\downarrow\downarrow$ phase would become locally unstable. The 10 SL $\uparrow\uparrow\uparrow\downarrow\downarrow$ phase remains locally stable only down to B_{c2}, where the frequency of a SW mode vanishes.

Our work demonstrates that the stacking of the hexagonal planes and the stability of a metamagnetic phase play crucial roles in determining the exchange and anisotropy parameters of a frustrated antiferromagnet. By constraining the fitting parameters at zero field, we have been able to identify the magnetic unit cell of the collinear metamagnetic phase in $CuFeO_2$. Constrained zero-field fits may prove to be a powerful technique for other systems as well.

We would like to acknowledge helpful conversations with Satoshi Okamoto. This research was sponsored by the Laboratory Directed Research and Development Program of Oak Ridge National Laboratory, managed by UT-Battelle, LLC for the U.S. Department of Energy under Contract No. DE-AC05-00OR22725, and by the Division of Materials Science and Engineering and the Division of Scientific User Facilities of the U.S. DOE.

[1] See, for example, *Frustrated Spin Systems*, edited by H. T. Diep (World Scientific, New Jersey, 2004).

[2] S. Mitsuda, H. Yoshizawa, N. Yaguchi, and M. Mekata, J. Phys. Soc. Jpn. **60**, 1885 (1991).

[3] M. Mekata, N. Yaguchi, T. Takagi, T. Sugino, S. Mitsuda, H. Yoshizawa, N. Hosoito, and T. Shinjo, J. Phys. Soc. Jpn. **62**, 4474 (1993).

[4] S. Mitsuda, T. Uno, M. Mase, H. Nojiri, K. Takahashi, M. Motokawa, and M. Arai, J. Phys. Chem. Solids **60**, 1249 (1999); S. Mitsuda, M. Mase, K. Prokes, H. Kitazawa, and H. A. Katori, J. Phys. Soc. Jpn. **69**, 3513 (2000).

[5] N. Terada, Y. Narumi, K. Katsumata, T. Yamamoto, U. Staub, K. Kindo, M. Hagiwara, Y. Tanaka, A. Kikkawa, H. Toyokawa, T. Fukui, R. Kanmuri, T. Ishikawa, and H. Kitamura, Phys. Rev. B **74**, 180404(R) (2006); N. Terada, Y. Narumi, Y. Sawai, K. Katsumata, U. Staub, Y. Tanaka, A. Kikkawa, T. Fukui, K. Kindo, T. Yamamoto, R. Kanmuri, M. Hagiwara, H. Toyokawa, T. Ishikawa, and H. Kitamura, *ibid.* **75**, 224411 (2007).

[6] T. Takagi and M. Mekata, J. Phys. Soc. Jpn. **64**, 4609 (1995).

[7] F. Ye, J. A. Fernandez-Baca, R. S. Fishman, Y. Ren, H. J. Kang, Y. Qiu, and T. Kimura, Phys. Rev. Lett. **99**, 157201 (2007); R. S. Fishman, J. Appl. Phys. **103**, 07B109 (2008).

[8] F. Wang and A. Vishwanath, Phys. Rev. Lett. **100**, 077201 (2008).

[9] N. Terada, S. Mitsuda, Y. Oohara, H. Yoshizawa, and H. Takei, J. Magn. Magn. Mater. **272–276**, E997 (2004); N. Terada, S. Mitsuda, K. Prokes, O. Suzuki, H. Kitazawa, and H. A. Katori, Phys. Rev. B **70**, 174412 (2004); N. Terada, S. Mitsuda, T. Fujii, and D. Petitgrand, J. Phys.: Condens. Matter **19**, 145241 (2007).

[10] O. A. Petrenko, M. R. Lees, G. Balakrishnan, S. de Brion, and G. Chouteau, J. Phys.: Condens. Matter **17**, 2741 (2005).

[11] S. Kanetsuki, S. Mitsuda, T. Nakajima, D. Anazawa, H. A. Katori, and K. Prokes, J. Phys.: Condens. Matter **19**, 145244 (2007).

[12] T. Kimura, J. C. Lashley, and A. P. Ramirez, Phys. Rev. B **73**, 220401(R) (2006).

[13] S. Seki, Y. Yamasaki, Y. Shiomi, S. Iguchi, Y. Onose, and Y. Tokura, Phys. Rev. B **75**, 100403(R) (2007).

[14] V. Eyert, R. Frésard, and A. Maignan, Phys. Rev. B **78**, 052402 (2008).

[15] M.-H. Whangbo, D. Dai, K.-S. Lee, and R. K. Kremer, Chem. Mater. **18**, 1268 (2006).

[16] F. Ye, Y. Ren, Q. Huang, J. A. Fernandez-Baca, P. Dai, J. W. Lynn, and T. Kimura, Phys. Rev. B **73**, 220404(R) (2006).